

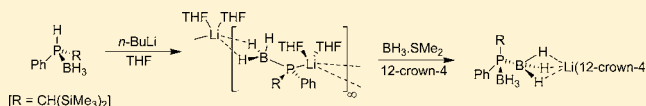
Phosphido-Borane and Phosphido-Bis(Borane) Complexes of the Alkali Metals, a Comparative Study

Keith Izod,* James M. Watson, William Clegg, and Ross W. Harrington

Main Group Chemistry Laboratories, School of Chemistry, Bedson Building, Newcastle University, Newcastle upon Tyne, NE1 7RU, U.K.

Supporting Information

ABSTRACT: Treatment of the secondary phosphine $\{(\text{Me}_3\text{Si})_2\text{CH}\}(\text{Ph})\text{PH}$ with $\text{BH}_3\cdot\text{SMe}_2$ yields the phosphine-borane $\{(\text{Me}_3\text{Si})_2\text{CH}\}(\text{Ph})\text{PH}(\text{BH}_3)$ (**12**) as colorless crystals. The reactions between **12** and $n\text{-BuLi}$, PhCH_2Na or PhCH_2K yield the corresponding phosphido-borane complexes $[[\{(\text{Me}_3\text{Si})_2\text{CH}\}(\text{Ph})\text{P}(\text{BH}_3)]\text{Li}(\text{THF})_2]_\infty$ (**13**), $[\{(\text{Me}_3\text{Si})_2\text{CH}\}(\text{Ph})\text{P}(\text{BH}_3)][\text{Na}(12\text{-crown-4})_2]$ (**14**), or $[[\{(\text{Me}_3\text{Si})_2\text{CH}\}(\text{Ph})\text{P}(\text{BH}_3)]\text{K}(\text{pmdeta})_2]$ (**15**), respectively, after crystallization in the presence of the appropriate co-ligand. While **13** crystallizes as a chain polymer, **14** crystallizes as a separated ion pair and **15** as a dimer. In both **13** and **15** the phosphido-borane ligands bind the alkali metal cations via both P–M and B–H...M contacts. Unexpectedly, NMR spectroscopy suggests that the separated ion pair **14** undergoes rapid inversion at phosphorus, while **13** and **15** do not. The phosphido-bis(borane) complexes $[\{(\text{Me}_3\text{Si})_2\text{CH}\}(\text{Ph})\text{P}(\text{BH}_3)_2]\text{Li}(12\text{-crown-4})$ (**16b**), $[[\{(\text{Me}_3\text{Si})_2\text{CH}\}(\text{Ph})\text{P}(\text{BH}_3)_2]\text{Na}(\text{THF})_2]_2$ (**17**), and $[[\{(\text{Me}_3\text{Si})_2\text{CH}\}(\text{Ph})\text{P}(\text{BH}_3)_2]\text{K}(\text{THF})_{0.5}]_\infty$ (**18a**) were prepared by treatment of the corresponding in situ-generated phosphido-borane complexes with $\text{BH}_3\cdot\text{SMe}_2$ and crystallization in the presence of the appropriate co-ligand. Compound **16b** crystallizes as a monomer, while **17** crystallizes as a dimer and **18a** crystallizes as a ribbon polymer. These crystallographic studies reveal entirely new binding modes for both phosphido-borane and phosphido-bis(borane) ligands and allow a direct comparison between these two ligand types.



INTRODUCTION

In spite of the isoelectronic relationship between silyl ligands, R_3Si^- , and phosphido-borane anions, $\text{R}_2\text{P}(\text{BH}_3)^-$, the latter compounds (also known as mono(borane)phosphides or phosphanylborohydrides) have received relatively little attention. This is particularly surprising given the relatively straightforward synthesis of these compounds and their potential utility: phosphido-boranes are key intermediates in the synthesis of novel (chiral) phosphines and in the catalytic dehydrocoupling of phosphine-boranes to give polymeric materials.^{1,2} Very recently, Gaumont and co-workers have shown that copper(I) phosphido-borane complexes are pre-catalysts for the formation of P–C(sp) bonds.³ Frequently, in these applications, the phosphido-borane intermediates are generated and used in situ; few such compounds have been isolated in the solid state. Those phosphido-borane complexes which have been isolated and structurally characterized may be divided into two classes: alkali metal complexes in which the hard metal center is coordinated principally by the borane hydrogen atoms of the ligand,⁴ and transition metal complexes in which the phosphido-borane ligand binds the softer metal center via its phosphorus donor atom.^{2,3,5} In this regard, it is notable that a recent report indicates that the lithium phosphido-borane complex $[\text{Ph}_2\text{P}(\text{BH}_3)]\text{Li}$ exhibits ditopic character.⁶ This compound reacts with aldehydes at low temperature to give the corresponding phosphine-borane-substituted alcohols (i.e., the phosphido-borane undergoes 1,2-addition across the C=O bond), while at higher temper-

atures the same reaction yields the phosphine-free secondary alcohols (i.e., the phosphido-borane anion acts as a hydride transfer reagent).

Even less numerous are complexes of phosphido-bis(borane) anions, $\text{R}_2\text{P}(\text{BH}_3)_2^-$, which are typically prepared by the addition of BH_3 to an alkali metal phosphido-borane complex, and which are the isoelectronic, negatively charged analogues of silanes. To date, only three such compounds have been structurally characterized, namely, $\{\text{R}_2\text{P}(\text{BH}_3)_2\}\text{K}(18\text{-crown-6})$ [$\text{R} = \text{Ph}$ (**1**), $t\text{-Bu}$ (**2**)]^{4b,7} and $\{(2,4,6\text{-}t\text{-Bu}_3\text{C}_6\text{H}_2)\text{PH}(\text{BH}_3)_2\}\text{Li}(\text{THF})_3$ (**3**);⁸ all three compounds crystallize as contact ion pairs in which the alkali metal cations are coordinated by the ether or tetrahydrofuran (THF) co-ligands and by only one of the BH_3 groups of the phosphido-bis(borane) ligand. In addition, Lancaster and co-workers have reported the crystal structure of the mixed phosphido-bis(borane) complex $[\text{Ph}_2\text{P}\{\text{B}(\text{C}_6\text{F}_5)_3\}(\text{BH}_3)]\text{Li}(\text{Et}_2\text{O})_3$ (**4**),⁹ while Bertrand and co-workers have reported the crystal structure of the unusual hydride-bridged complex $[\{(2,4,6\text{-}t\text{-Bu}_3\text{C}_6\text{H}_2)\text{P}(\text{BH}_3)\{\mu\text{-BH}_2\}_2\text{H}\}]\text{Li}(\text{THF})_2]_2$.⁸

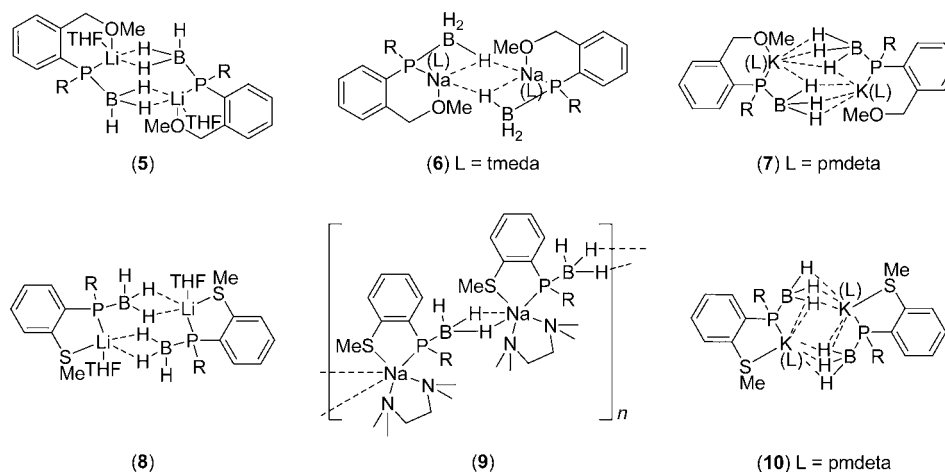
We recently reported the synthesis and crystal structures of a series of alkali metal phosphido-borane complexes possessing peripheral donor functionalization through the incorporation of a benzyl ether or thioether group in the ligand (**5–10**, Chart 1).^{10,11} This donor functionalization leads to additional M–O

Received: October 10, 2012

Published: January 15, 2013

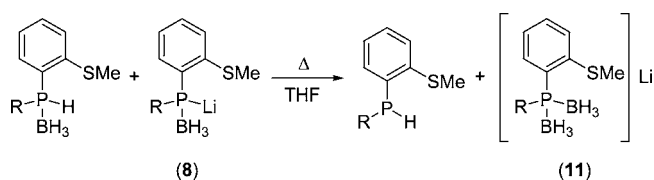


Chart 1



or M–S interactions and the consequent formation of chelate rings in their complexes. For the thioether-functionalized ligands we noted a borane-redistribution reaction between the lithium phosphido-borane complex (8) and free phosphine-borane, which yields a phosphido-bis(borane) complex (11) and free secondary phosphine (Scheme 1);¹⁰ however,

Scheme 1



although we subsequently prepared 11 by a more logical route (addition of BH_3SMe_2 to the phosphido-borane 8), we were not able to obtain any suitable crystals of this compound to investigate its structure.

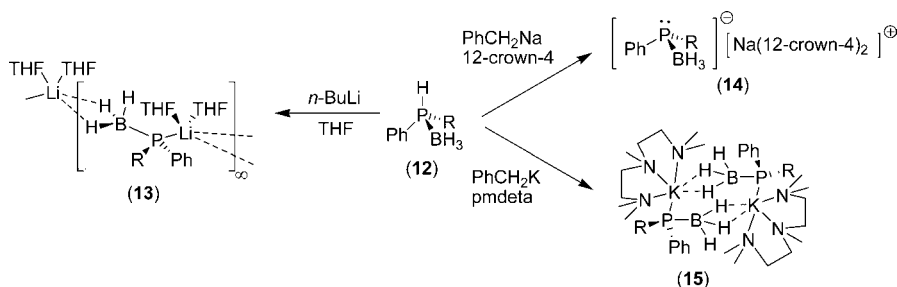
We now report the synthesis and structural characterization of a new phosphine-borane, free from peripheral donor functionalization, its lithium, sodium, and potassium derivatives, and their conversion into the corresponding phosphido-bis(borane) complexes. This provides the first opportunity to compare the coordination behavior of phosphido-borane and phosphido-bis(borane) ligands within a closely related family of compounds.

RESULTS AND DISCUSSION

The reaction between $\{(\text{Me}_3\text{Si})_2\text{CH}\}(\text{Ph})\text{PH}^{12}$ and 1 equiv of BH_3SMe_2 in THF gives the phosphine-borane $\{(\text{Me}_3\text{Si})_2\text{CH}\}$ -

$(\text{Ph})\text{PH}(\text{BH}_3)$ (12), after removal of volatiles, as a colorless, crystalline solid in good yield. Treatment of a solution of 12 in THF with 1 equiv of *n*-BuLi leads to rapid deprotonation and the formation of the lithium complex $[\{(\text{Me}_3\text{Si})_2\text{CH}\}(\text{Ph})\text{P}(\text{BH}_3)]\text{Li}(\text{THF})_2]_\infty$ (13), which crystallizes from methylcyclohexane/THF as colorless blocks (Scheme 2). Similarly, the reaction between 12 and 1 equiv of either PhCH_2Na or PhCH_2K in THF gives the corresponding heavier alkali metal phosphido-borane complexes, which are isolated as the separated ion pair $[\{(\text{Me}_3\text{Si})_2\text{CH}\}(\text{Ph})\text{P}(\text{BH}_3)][\text{Na}(12\text{-crown-4})_2]$ (14) and the dimer $[\{(\text{Me}_3\text{Si})_2\text{CH}\}(\text{Ph})\text{P}(\text{BH}_3)]\text{K}(\text{pmdeta})_2$ (15), respectively, in good yields, after crystallization in the presence of the appropriate co-ligand [pmdeta = *N,N,N',N',N''*-pentamethyldiethylenetriamine].

Upon metalation, the $^{31}\text{P}\{^1\text{H}\}$ NMR signal observed for 12 (-8.6 ppm) moves to significantly higher field [-56.8 (13), -41.0 (14), -50.6 (15) ppm]. In our previous studies on phosphido-borane complexes we have found the $^{31}\text{P}\{^1\text{H}\}$ chemical shifts to be essentially independent of the nature of the alkali metal cation;^{10,11} however, each of the compounds in our earlier studies crystallizes as a contact ion pair. We attribute the somewhat lower-field chemical shift of 14 compared to 13 and 15 to the formation of a separated ion pair in the former compound. The ^{31}P - ^{11}B coupling constants of 12–15 exhibit a significant decrease with increasing ionic character of the P–H/M bond [$J_{\text{PB}} = 52$ (12), 44 (13), 26 (14), 20 (15) Hz]. This is consistent with Bent's rule:¹³ increasing ionic character leads to increasing phosphorus *s*-character in the P–H/M bond and thus increasing *p*-character in the P–B bond; this results in a decrease in the Fermi contact term and so a decrease in the ^{31}P - ^{11}B coupling constant. The rather similar ^{31}P - ^{11}B coupling

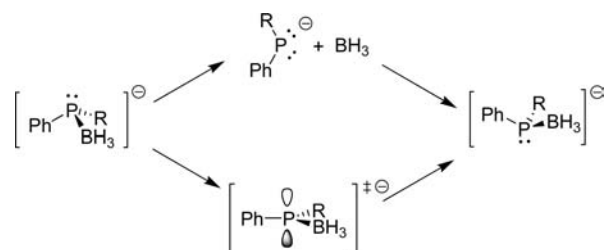
Scheme 2. [R = $\text{CH}(\text{SiMe}_3)_2$]

constants of the potassium complex **15** and the separated ion pair **14** suggest that the P–K bonding in the former is essentially ionic in nature. Coupling between ^{31}P and ^7Li is not observed in **13**, indicating rapid exchange on the NMR time-scale.

The room-temperature ^1H NMR spectra of the contact ion pairs **13** and **15** in d_8 -THF are as expected and are consistent with the above formulations: the diastereotopic SiMe_3 groups give rise to a pair of singlets in each case at 0.29 and 0.39 ppm (**13**) and 0.28 and 0.42 ppm (**15**), respectively, and the ^1H NMR spectra of **13** and **15** do not vary with temperature. Unexpectedly, however, in the room-temperature ^1H NMR spectrum of **14** in d_8 -THF the SiMe_3 groups appear as two rather broad singlets. At lower temperatures these signals sharpen, such that, below $-10\text{ }^\circ\text{C}$, two sharp singlets are observed at -0.09 and 0.15 ppm; at temperatures above ambient these signals broaden and coalesce until, at $55\text{ }^\circ\text{C}$, a broad singlet at 0.10 ppm is observed. The remaining signals are unaffected by temperature.

This behavior may be attributed to a dynamic equilibrium which interconverts the two diastereotopic SiMe_3 groups and suggests that, at ambient temperature and above, **14** is subject to rapid inversion at the phosphorus center. Such an inversion process may reasonably occur via one of two distinct mechanisms: (i) dissociation of the borane group and subsequent re-coordination at phosphorus to give the alternative enantiomeric form, or (ii) inversion at phosphorus via a planar transition state (Scheme 3). With regard to the first

Scheme 3



mechanism, Imamoto and co-workers have suggested that the racemization of *o*-anisyl-substituted tertiary phosphine-boranes occurs via a dynamic equilibrium in which the anisyl oxygen atom abstracts the borane group from phosphorus, generating an intermediate tertiary phosphine, which then racemizes prior to re-coordination of the borane group.¹⁴ In light of this, it is feasible that the dissociation of BH_3 from **14** to form a two-coordinate (achiral) phosphide anion would be assisted by the formation of a THF-BH_3 adduct, reducing the barrier to dissociation. However, theoretical calculations yield a bond dissociation energy of 166.5 kJ mol^{-1} for the neutral phosphine-borane adduct $\text{Me}_3\text{P-BH}_3$,¹⁵ and it is likely that the negative charge localized on phosphorus in **14** would increase the strength of the P–B σ -bond, and so rapid dissociation of BH_3 from **14** appears unlikely. In this regard, line-shape analysis of the variable-temperature ^1H NMR spectra of **14** gives values of $\Delta H^\ddagger = 52.8 \pm 5.0\text{ kJ mol}^{-1}$ and $\Delta S^\ddagger = -28 \pm 10\text{ J K}^{-1}\text{ mol}^{-1}$, and consequently $\Delta G^\ddagger = 61.1 \pm 5.0\text{ kJ mol}^{-1}$, for this process at 298 K , substantially less than the likely P–B bond dissociation energy.

The alternative mechanism for the inversion of **14** involves a trigonal planar transition state. Although calculations indicate that the barrier to inversion at phosphorus via such a transition

state is rather large, and hence chiral tertiary phosphines (and, by inference, chiral phosphido-borane anions) are largely configurationally stable,¹⁶ it has been reported that the presence of electropositive substituents acts to greatly reduce this barrier.^{16,17} For example, the inversion barriers for $i\text{PrPhP}(\text{EMe}_3)$ have been measured as 136.8 , 89.5 , and 80.8 kJ mol^{-1} for $\text{E} = \text{C}$, Ge , and Sn , respectively.¹⁷ With particular relevance to the current system, we have shown that inversion at phosphorus in the phosphatetrylenes $[\{(\text{Me}_3\text{Si})_2\text{CH}\}\text{P}(\text{C}_6\text{H}_4\text{-}2\text{-CH}_2\text{NMe}_2)]\text{ECl}$ and $[\{(\text{Me}_3\text{Si})_2\text{CH}\}\text{P}(\text{C}_6\text{H}_4\text{-}2\text{-CH}_2\text{NMe}_2)]_2\text{E}$ ($\text{E} = \text{Ge}$, Sn) is rapid on the NMR time-scale.¹⁸ Calculations on the model phosphatetrylenes $[\text{MeP}(\text{C}_6\text{H}_4\text{-}2\text{-CH}_2\text{NMe}_2)]\text{GeX}$ ($\text{X} = \text{F}$, Cl , Br , H , Me) indicate that the barrier to inversion at phosphorus via a planar transition state ranges from 66.1 to 98.7 kJ mol^{-1} , depending on the substituent X .¹⁹ The Pauling electronegativity of boron (2.04) is similar to that of germanium (2.01) and so a borane group should exert an influence over the inversion barrier of phosphorus similar to that of a germyl group. We note that the barrier to inversion at phosphorus calculated for $[\text{MeP}(\text{C}_6\text{H}_4\text{-}2\text{-CH}_2\text{NMe}_2)]\text{GeF}$ (66.1 kJ mol^{-1}) lies close to that observed for **14** and so tentatively favor this mechanism as an explanation for the high-temperature equivalence of the diastereotopic SiMe_3 groups in the latter compound. The temperature-invariant nature of the ^1H NMR spectra of **13** and **15** indicates that, where the cation is not fully separated from the anion, inversion at phosphorus is inhibited.

To provide a comparison with the metalated derivatives we obtained an X-ray crystal structure of the free phosphine-borane **12**; the molecular structure of **12** is shown in Figure 1,

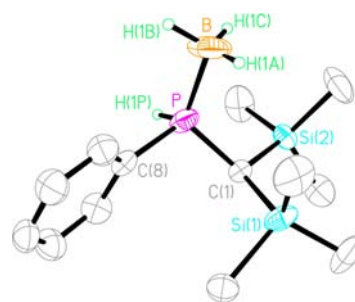


Figure 1. Molecular structure of **12** with C-bound H atoms and the minor disorder component omitted for clarity. Selected bond lengths (Å) and angles (deg): P–H(1P) $1.35(4)$, P–B $1.920(7)$, P–C(1) $1.814(4)$, P–C(8) $1.805(4)$, C(1)–Si(1) $1.898(4)$, C(1)–Si(2) $1.910(4)$, B–H(1A) $1.17(6)$, B–H(1B) $1.04(6)$, B–H(1C) $1.04(5)$, B–P–C(1) $117.7(3)$, B–P–C(8) $113.9(3)$, C(1)–P–C(8) $108.34(17)$.

along with selected bond lengths and angles. The P–C(1), P–C(8), and P–B distances [$1.814(4)$, $1.805(4)$, and $1.920(7)$ Å, respectively] are similar to the corresponding distances in previously reported phosphine-borane adducts; the sum of angles in the C_2PB core is 339.9° .

The lithium complex **13** crystallizes as infinite chains of alternating lithium cations and phosphido-borane anions; the structure of **13** is shown in Figure 2, along with selected bond lengths and angles. Each lithium cation is coordinated by the phosphorus atom of one phosphido-borane ligand and, in an η^2 -manner, by two borane hydrogen atoms of an adjacent phosphido-borane ligand in the chain. The coordination of each lithium ion is completed by two molecules of THF. Thus, each phosphido-borane anion bridges adjacent lithium cations via its

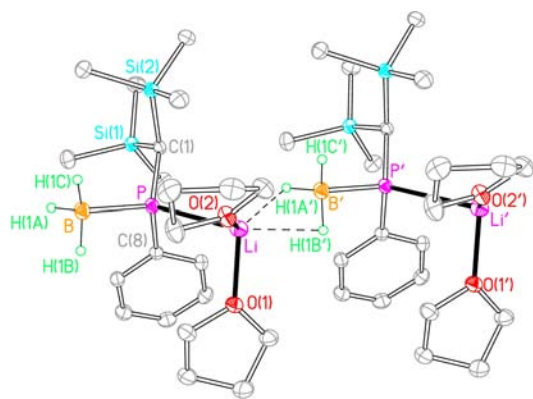


Figure 2. Section of the structure of polymeric **13** with C-bound H atoms omitted for clarity. Selected bond lengths (Å) and angles (deg): Li–P 2.741(3), Li–H(1A′) 2.086(18), Li–H(1B′) 2.183(19), Li···H(1C′) 2.79(2), Li···B′ 2.440(3), Li–O(1) 1.985(3), Li–O(2) 1.949(3), P–B 1.9611(17), P–C(1) 1.8851(14), P–C(8) 1.8395(14), B–P–C(1) 110.55(7), B–P–C(8) 106.09(7), C(1)–P–C(8) 102.95(6). Primed atoms are related by the symmetry operator $x-1, y, z$ (translation by one unit cell along the a axis).

P and BH_3 centers. The P–Li distance of 2.741(3) Å is somewhat longer than the corresponding distances in **5** and **8** [2.611(6) and 2.527(3) Å, respectively],^{10,11} reflecting the fact that the P–Li bond is incorporated into a chelate ring in the latter two compounds. Indeed, the P–Li distance in **13** is significantly longer than the corresponding distance in $[\{\text{Me}_2\text{P}(\text{BH}_3)\}\text{Li}(\text{tmeda})]_\infty$ [2.620(4) Å],^{4a} which is, with the exception of **5** and **8**, the only other lithium complex of a phosphido-borane anion, and lies at the longer end of the range of typical P–Li distances in lithium phosphides $(\text{R}_2\text{P})\text{Li}[\text{tmeda} = N,N,N',N'$ -tetramethylethylenediamine].²⁰ The Li–H distances [2.086(18) and 2.183(19) Å] and the Li···B distance [2.440(3) Å] are typical of $\eta^2\text{-BH}_n\text{-Li}$ contacts. For example, the Li–H and Li···B distances in $[\{\text{Me}_2\text{P}(\text{BH}_3)\}\text{Li}(\text{tmeda})]_\infty$ are 2.03(2) and 2.372(4) Å, respectively,^{4a} while the Li–H and Li···B distances in **5** are 1.99(4) and 2.05(4) Å and 2.453(7) Å, respectively.¹⁰ The next shortest Li···H(B) distance in **13** is 2.79(2) Å, so that an η^3 formulation is not appropriate.

Metalation of **12** results in a significant lengthening of the P–B bond from 1.920(7) Å in **12** to 1.9611(17) Å in **13**; similarly the P–C(1) and P–C(2) distances increase from 1.814(4) and 1.805(4) Å in **12** to 1.8851(14) and 1.8395(14) Å in **13**, respectively. Metalation also leads to increasing pyramidalization at phosphorus: in **12** the sum of angles within the C_2PB framework is 339.9°, whereas the sum of angles at phosphorus in **13** is 319.6°.

The polymeric chains of **13** pack such that the phenyl rings are oriented toward each other; however, there are no significant π -stacking interactions between the rings, which are arranged in a substantially offset inter-digitated fashion along the chains.

In contrast to the polymeric structure of **13**, compound **14** crystallizes as a separated ion pair; this permits a direct comparison of the structure of the isolated phosphido-borane anion with those of its lithium complex and of the parent phosphine-borane **12**. The structure of **14** is shown in Figure 3, along with selected bond lengths and angles. The $[\text{Na}(12\text{-crown-4})_2]^+$ cation is unexceptional and requires no further comment.

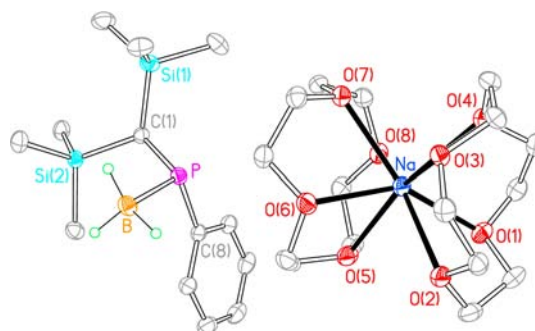


Figure 3. Structure of **14** with C-bound H atoms omitted for clarity. Selected bond lengths (Å) and angles (deg): Na–O 2.466 (average), P–B 1.9688(15), P–C(1) 1.8899(13), P–C(8) 1.8400(14), B–P–C(1) 110.57(6), B–P–C(8) 106.06(7), C(1)–P–C(8) 101.50(6).

The P–B, P–C(1), and P–C(8) distances in **14** [1.9688(15), 1.8899(13), and 1.8400(14) Å, respectively] are almost identical to the corresponding distances in **13** [1.9611(17), 1.8850(14), and 1.8394(14) Å, respectively], while the sum of angles in the PBC₂ framework in **14** [318.67°] is also very similar to that for **13** [319.60°]. This clearly implies that coordination of the lithium cation in **13** has little impact on the bonding in the phosphido-borane anion itself.

In contrast to **13** and **14**, the potassium salt **15** crystallizes as a discrete molecular species; the molecular structure of **15** is shown in Figure 4, along with selected bond lengths and angles.

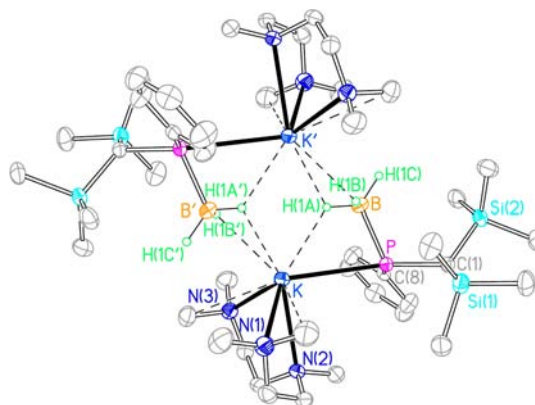


Figure 4. Structure of **15** with C-bound H atoms omitted for clarity. Selected bond lengths (Å) and angles (deg): P–B 1.969(3), P–C(1) 1.874(2), P–C(8) 1.831(2), K–P 3.2754(8), K–H(1A) 2.71(2), K–H(1A′) 2.76(2), K–H(1B′) 2.77(3), K···H(1B) 3.22(3), K···H(1C′) 3.25(3), K···B 3.262(3), K···B′ 3.107(3), K–N(1) 2.830(2), K–N(2) 2.9132(18), K–N(3) 2.801(2), K···C(15) 3.275(4), K···C(22) 3.418(3), P–K···B 35.06(5), B···K···B′ 96.32(7), K···B···K′ 83.69(7), B–P–C(1) 111.20(11), B–P–C(8) 107.46(12), C(1)–P–C(8) 102.57(10). Primed atoms are related by the inversion operator $1-x, 1-y, 1-z$.

Compound **15** crystallizes as a dimer in which each potassium ion is bound by the phosphorus atom and one of the borane hydrogen atoms of a phosphido-borane ligand; this “side-on” coordination mode closely resembles the P,B binding mode observed in the related potassium complex $[\text{Ph}_2\text{P}(\text{BH}_3)]\text{K}(18\text{-crown-6})$.^{4c} The coordination sphere of each potassium ion in **15** is completed by the three nitrogen atoms of a molecule of pmdeta , an $\eta^2\text{-BH}_3$ group from the second phosphido-borane ligand in the dimer, and two short $\text{K}\cdots\text{Me}$ contacts to two of the methyl groups of the tmeda co-ligand. Thus, the borane

groups act as $\mu_2\text{-}\eta^1\text{:}\eta^2$ -bridges between the two potassium ions in the dimer, generating a planar $\text{K}_2(\text{BH}_3)_2$ rhombus-shaped core. The next shortest $\text{K}\cdots\text{H}(\text{B})$ distances are 3.22(3) and 3.25(3) Å, almost 0.5 Å longer than the most significant interactions described here.

The K-P distance of 3.2754(8) Å in **15** is somewhat shorter than the corresponding distance in $[\text{Ph}_2\text{P}(\text{BH}_3)]\text{K}(\text{18-crown-6})$ [3.320(2) Å]^{4c} and is substantially shorter than the corresponding distances in the closely related compounds **7** and **10** [K-P 3.7619(10) and 3.6617(6) Å, respectively].^{10,11} In contrast, the $\text{K}\cdots\text{B}$ distance of 3.262(3) Å in **15** is slightly longer than the corresponding distance in $[\text{Ph}_2\text{P}(\text{BH}_3)]\text{K}(\text{18-crown-6})$ [3.162 Å], which also exhibits an $\eta^2\text{-BH}_3$ binding mode, but is similar to the corresponding distances in **7** and **10** [$\text{K}\cdots\text{B}$ 3.322(3) and 3.234(2) Å, respectively].

Since phosphido-borane ligands $\text{RR}'\text{P}(\text{BH}_3)^-$ are isoelectronic with the corresponding methyl-substituted silyl ligands $\text{RR}'\text{SiMe}^-$, it is pertinent to compare the structures of their alkali metal derivatives. While the compounds $[\{(\text{Me}_3\text{Si})_2\text{CH}\}(\text{Ph})(\text{Me})\text{Si}\}\text{M}$ [$\text{M} = \text{Li}, \text{Na}, \text{K}$] are unknown and so a direct comparison with the structures of these species is not possible, several alkali metal complexes of methyl-substituted silyl ligands have been crystallographically characterized.²¹ Typically, in these compounds the alkali metal is coordinated by the silicon center of the silyl ligand, along with the donor atoms of any coligands, and, in some cases, these contacts are supplemented by weak $\text{C-H}\cdots\text{M}$ contacts with organic groups at the periphery of the molecule. For example, in the complex $[(\text{Me}_3\text{Si})_2(\text{Me})\text{Si}]\text{K}(\text{PhH})_2$,^{21a} alongside the K-Si contact, there are short contacts between the potassium ion and two η^6 -benzene molecules along with short $\text{C-H}\cdots\text{K}$ contacts between the potassium ion and a methyl group on two of the *t*-Bu substituents of the silyl ligand; there are no short contacts in this complex between the potassium ion and the Si-Me group. To the best of our knowledge, the only crystallographically characterized $\text{Si-Me}\cdots\text{M}$ contact, where the silicon center bears a negative charge, is found in the mixed aggregate $[\{[(t\text{-BuMe}_2\text{Si})_2\text{Si}]\text{Li}_2\}_2\{(t\text{-BuMe}_2\text{Si})\text{Li}\}_2]$,^{21b} in which the $\text{Li}\cdots\text{C}$ distance is 2.355 Å [cf. $\text{Li}\cdots\text{B}$ 2.440(3) in **13**]. This contrasts with the prevalence of $\text{P-BH}_3\cdots\text{M}$ contacts found in phosphido-borane complexes of the alkali metals, clearly illustrating the greater hydridic character of P-BH_3 compared to Si-CH_3 hydrogen atoms.

We noted above the scarcity of well-characterized complexes of phosphido-bis(borane) anions. This is particularly surprising given that these anions are direct homologues of the amido-bis(borane) ligands developed by Nöth and subsequently employed by Girolami and co-workers for the synthesis of a range of highly volatile, high coordination number lanthanide and actinide compounds.^{22,23} We previously observed that thermolysis of **7** in the presence of free phosphine-borane leads to a borane-redistribution reaction, ultimately yielding the corresponding alkali metal phosphine-bis(borane) (**11**) and free secondary phosphine (Scheme 1).¹⁰ Although we were unable to crystallize **11** its constitution was unambiguously verified by NMR spectroscopy.

To gain more insight into the structures and binding modes of this under-developed ligand class, we sought to prepare the phosphido-bis(borane) analogues of **13–15**. Treatment of a solution of **13** in THF with 1 equiv of $\text{BH}_3\cdot\text{SMe}_2$ gives the phosphido-bis(borane) complex $[\{(\text{Me}_3\text{Si})_2\text{CH}\}(\text{Ph})\text{P}(\text{BH}_3)_2]\text{Li}(\text{THF})_n$ (**16a**). Although we were unable to crystallize this compound, treatment of a solution of **16a** in

toluene with 1 equiv of 12-crown-4 gave the adduct $[\{(\text{Me}_3\text{Si})_2\text{CH}\}(\text{Ph})\text{P}(\text{BH}_3)_2]\text{Li}(\text{12-crown-4})$ (**16b**), which was crystallized from cold toluene as colorless blocks suitable for X-ray crystallography. The ^1H and $^{13}\text{C}\{^1\text{H}\}$ NMR spectra of **16b** are consistent with the proposed formulation; the $^{31}\text{P}\{^1\text{H}\}$ spectrum consists of a broad, unresolved multiplet at -8.8 ppm due to coupling to two quadrupolar ^{11}B nuclei, while the $^{11}\text{B}\{^1\text{H}\}$ spectrum exhibits a broad doublet ($J_{\text{PB}} = 46$ Hz) at -32.5 ppm.

The sodium analogue $[\{[(\text{Me}_3\text{Si})_2\text{CH}\}(\text{Ph})\text{P}(\text{BH}_3)_2]\text{Na}(\text{THF})_2\}_2$ (**17**) was synthesized by the reaction of **12** with benzylsodium and subsequent treatment with 1 equiv of $\text{BH}_3\cdot\text{SMe}_2$; single crystals were obtained from a cold mixture of methylcyclohexane, toluene, and THF (10:2:5). The corresponding potassium salt $[\{[(\text{Me}_3\text{Si})_2\text{CH}\}(\text{Ph})\text{P}(\text{BH}_3)_2]\text{K}(\text{THF})_{0.5}\}_\infty$ (**18a**) was prepared by a similar reaction between **12**, benzylpotassium, and $\text{BH}_3\cdot\text{SMe}_2$ in THF and was crystallized from cold toluene/THF; a second batch of crystals, obtained in a similar fashion, proved to be of the alternative solvate $[\{[(\text{Me}_3\text{Si})_2\text{CH}\}(\text{Ph})\text{P}(\text{BH}_3)_2]\text{K}(\text{THF})_2\}_\infty \cdot 1/2\text{PhMe}]$ (**18b**). The ^1H , $^{13}\text{C}\{^1\text{H}\}$, $^{11}\text{B}\{^1\text{H}\}$, and $^{31}\text{P}\{^1\text{H}\}$ NMR spectra of **17** and **18** are as expected; the $^{11}\text{B}\{^1\text{H}\}$ spectra of **17** and **18** consist of broad doublets at -33.8 ($J_{\text{BP}} = 69$ Hz) and -32.9 ppm ($J_{\text{BP}} = 64$ Hz), respectively, while the $^{31}\text{P}\{^1\text{H}\}$ NMR spectra consist of broad, unresolved multiplets at -14.9 and -14.1 ppm, respectively.

The structure of **16b** is shown in Figure 5, along with selected bond lengths and angles. Compound **16b** crystallizes

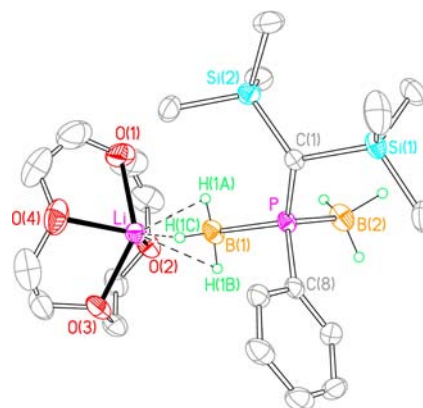


Figure 5. Structure of **16b** with C-bound H atoms and the minor disorder component omitted for clarity. Selected bond lengths (Å) and angles (deg): $\text{Li-H}(1\text{A})$ 2.01(4), $\text{Li-H}(1\text{B})$ 2.28(5), $\text{Li-H}(1\text{C})$ 2.27(5), $\text{Li}\cdots\text{B}$ 2.281(8), $\text{Li-O}(1)$ 2.157(8), $\text{Li-O}(2)$ 2.072(8), $\text{Li-O}(3)$ 2.090(7), $\text{Li-O}(4)$ 2.129(8), $\text{P-B}(1)$ 1.929(4), $\text{P-B}(2)$ 1.948(5), $\text{P-C}(1)$ 1.854(3), $\text{P-C}(8)$ 1.832(4), $\text{B}(1)\text{-P-B}(2)$ 111.0(2), $\text{B}(1)\text{-P-C}(1)$ 115.39(19), $\text{B}(1)\text{-P-C}(8)$ 102.48(18), $\text{B}(2)\text{-P-C}(1)$ 111.68(18), $\text{B}(2)\text{-P-C}(8)$ 113.6(2), $\text{C}(1)\text{-P-C}(8)$ 102.20(16).

as discrete monomers in which the lithium ion is coordinated by the four oxygen atoms of a molecule of 12-crown-4 and, in an η^3 manner, by one of the two borane groups of the phosphido-bis(borane) ligand; the second borane group has no short contacts to lithium. The binding mode of the phosphido-bis(borane) ligand in **16b** is similar to that observed in the three previously reported alkali metal phosphido-bis(borane) complexes **1–3**.

The Li-H distances of 2.01(4), 2.28(5) and 2.27(5) Å and the $\text{Li}\cdots\text{B}$ distance of 2.281(8) Å are consistent with the η^3

binding mode of the borane group in **16b**; for example, the Li–H distances in $(4\text{-MeC}_3\text{H}_4\text{N})_3\text{Li}(\eta^3\text{-BH}_4)$ are 2.10(2), 2.20(2), and 2.10(2), while the Li⋯B distance in this compound is 2.319(5) Å.²⁴ The P–B(1) distance of 1.929(4) Å is slightly shorter than the “free” P–B(2) distance [1.948(5) Å], although it is difficult to attribute this to any steric or electronic effects; a similar difference between the P–B distances of the “free” and coordinated BH_3 groups was observed for **3**. However, both P–B distances in **16b** are significantly shorter than the P–B distances in **3** [1.955(3) and 1.984(3) Å], and in the phosphido-borane complexes **8** [1.9617(18) Å] and **13** [1.9611(17) Å].

In contrast to monomeric **16b**, compound **17** crystallizes as discrete dimers with a crystallographic inversion center midway along the Na⋯Na vector; the molecular structure of **17** is shown in Figure 6, along with selected bond lengths and angles.

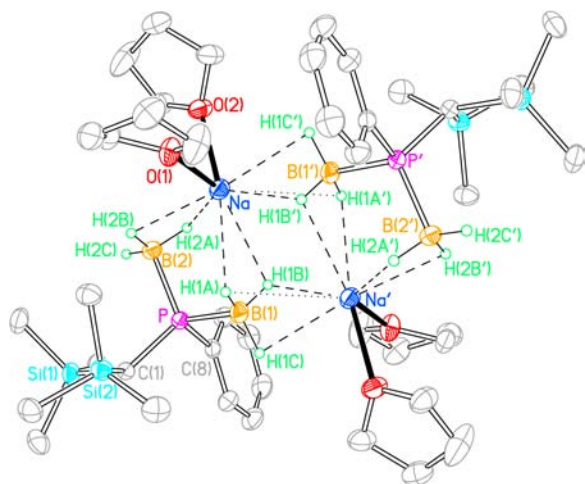


Figure 6. Structure of **17** with C-bound H atoms omitted for clarity. Selected bond lengths (Å) and angles (deg): Na–O(1) 2.339(2), Na–O(2) 2.369(2), Na–H(1A) 2.63(2), Na–H(1B) 2.67(3), Na–H(2A) 2.42(2), Na–H(2B) 2.54(3), Na–H(1B′) 2.42(3), Na–H(1C′) 2.59(3), Na⋯H(1A′) 2.95(3), Na⋯B(1) 3.011(3), Na⋯B(2) 2.864(3), Na⋯B(1′) 2.782(3), P–B(1) 1.950(3), P–B(2) 1.958(3), P–C(1) 1.862(2), P–C(8) 1.846(2), B(1)⋯Na⋯B(2) 65.79(8), B(1′)⋯Na⋯B(2) 144.87(9), B(1)⋯Na⋯B(1′) 88.88(9), Na⋯B(1)⋯Na′ 91.12(9). Primed atoms are related by the inversion symmetry operation $1-x, 1-y, 1-z$.

Each sodium ion is coordinated by two molecules of THF, two $\eta^2\text{-BH}_3$ groups from one phosphido-bis(borane) ligand and an $\eta^2\text{-BH}_3$ group from the second phosphido-bis(borane) ligand in the dimer. Thus, each phosphido-bis(borane) ligand chelates one sodium ion via two $\eta^2\text{-BH}_3\cdots\text{Na}$ contacts, while one of the BH_3 groups acts as an $\eta^2:\eta^2$ -bridge between the two sodium ions in the dimer. Neither chelating nor bridging bonding motifs have been observed previously for phosphido-bis(borane) ligands, although the related amido-bis(borane) ligands developed by Nöth and co-workers are known to adopt similar chelating modes.^{22,23} A slightly longer Na⋯H distance (by 0.28 Å, similar to the range of the primary Na–H distances) means that the links between the two halves of the dimer through the bridging borane group are actually intermediate between η^2 and η^3 , as shown in Figure 6.

The dimer is constructed around a central $\text{Na}_2(\text{BH}_3)_2$ rectangle with primary Na–H contacts ranging from 2.42(2) to 2.67(3) Å and Na⋯B distances of 3.011(3) and 2.782(3) Å.

These distances are similar to the corresponding distances in **6** [Na⋯B 2.987(5) and 2.845(5) Å] and in $(\text{py})_3\text{Na}(\eta^2\text{-BH}_4)$ [Na⋯B 2.927(3) Å].²⁵ The two P–B distances in **17** are essentially identical [1.950(3) and 1.958(3) Å] and are similar to those observed in **16b** and **3**.

Both **18a** and **18b** crystallize as ribbon-type polymers; the structures of **18a** and **18b** are shown in Figure 7, along with selected bond lengths and angles. These two compounds differ in the degree of solvation of the potassium ions: in **18a** half of the potassium ions in the chain are coordinated by a single molecule of THF each, while in **18b** each potassium ion is coordinated by two molecules of THF; additionally, the crystal of **18b** contains uncoordinated solvent, highly disordered, which is probably toluene. Nevertheless, the overall structures of both **18a** and **18b** are very similar.

In **18a**, allowing a generous range for K–H distances, each potassium ion is coordinated by two $\eta^2\text{-BH}_3$ groups from a chelating phosphido-bis(borane) ligand and two $\eta^3\text{-BH}_3$ groups from two adjacent phosphido-bis(borane) ligands in the chain; additionally, half of the potassium ions are each coordinated by one molecule of THF, the packing of the chains providing insufficient space for THF coordination of all the cations; the THF molecules are disordered over inversion centers located between the chains.

Compound **18b** crystallizes with a very similar structure to that of **18a**, but here each potassium ion is coordinated by two molecules of THF, in addition to the two $\eta^2\text{-BH}_3$ groups from a chelating phosphido-bis(borane) ligand and two $\eta^3\text{-BH}_3$ groups from adjacent phosphido-bis(borane) ligands in the chain. The greater mean K–H distance (and larger range of distances) in **18b** than in **18a** reflects the increased coordination by THF in the former compound.

The K–H and K⋯B distances in **18a** and **18b** [**18a**: K–H 2.698(18)–3.191(19) Å, K⋯B 3.039(2)–3.224(2) Å; **18b**: K–H 2.77(3)–3.40(3), K⋯B 3.132(4)–3.416(4) Å] are similar to the corresponding distances in previously reported phosphido-borane and phosphido-bis(borane) complexes of potassium. For example, the K–H distances in **7** range from 2.796(18) to 3.06(2) Å, while the K⋯B distances in this compound are 3.103(3) and 3.322(3) Å.

Comparison of the structures of the contact ion pair lithium phosphido-borane and phosphido-bis(borane) complexes **13** and **16b** reveals that, while there is little difference in the Li–H distances in these two compounds [Li–H 2.086(18), 2.183(19) Å (**13**); 2.01(4), 2.27(5), 2.28(5) Å (**16b**)], the P–B distance in **13** [1.9611(17) Å] is somewhat longer than the corresponding distances in **16b** [1.929(4) and 1.948(5) Å]. Furthermore, while the K–H distances in **15** and **18a** are also rather similar, the P–B distance in the potassium phosphido-borane complex **15** [1.969(3) Å] is significantly longer than the P–B distances in the potassium phosphido-bis(borane) complex **18a** [1.940(2) and 1.941(2) Å]. This is a reflection of the increased phosphorus p-character in the P–B bonds in **13** and **15**, which arises from the highly ionic nature and consequent high phosphorus s-character of the P–Li and P–K bonds in these compounds.

CONCLUSIONS

Phosphido-boranes $\text{R}_2\text{P}(\text{BH}_3)^-$ represent a versatile class of potentially ambidentate and/or polydentate anionic ligand. While these ligands may adopt a wide variety of coordination modes there appears to be a marked preference for the formation of $\text{BH}_3\cdots\text{M}$ contacts in their complexes with hard

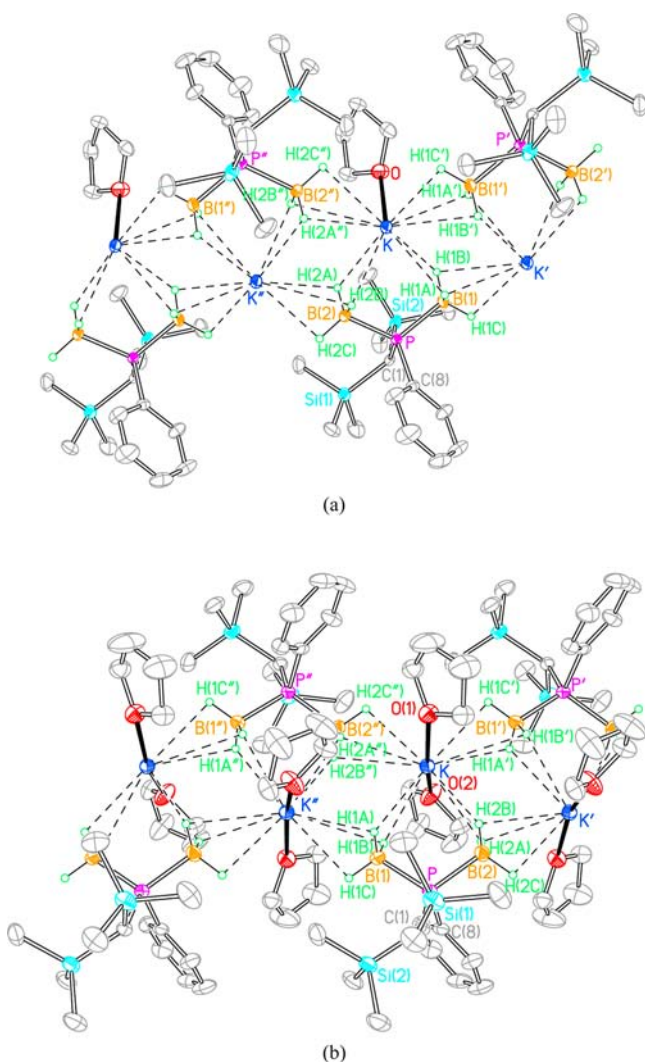


Figure 7. (a) Structure of **18a** and (b) structure of **18b** with C-bound H atoms omitted for clarity. Selected bond lengths (Å) and angles (deg) for **18a**: K–O 2.762(3), K–H(1A) 2.813(18), K–H(1B) 2.78(2), K–H(2A) 2.822(19), K–H(2B) 2.698(18), K–H(1A') 2.766(18), K–H(1B') 3.191(19), K–H(1C') 2.762(18), K–H(2A'') 2.924(18), K–H(2B'') 3.084(18), K–H(2C'') 2.79(2), K···B(1) 3.224(2), K···B(2) 3.174(2), K···B(1') 3.039(2), K···B(2') 3.083(2), P–B(1) 1.941(2), P–B(2) 1.940(2), P–C(1) 1.8410(16), P–C(8) 1.8326(16), K···B(1)···K' 93.06(5), K···B(2)···K'' 889.59(5). Primed and double-primed atoms are related by the inversion symmetry operators $-x, -y, 1-z$ and $1-x, -y, 1-z$, respectively. For **18b**: K–O(1) 2.730(2), K–O(2) 2.735(2), K–H(1A) 3.05(3), K–H(1B) 2.77(3), K–H(2A) 2.89(3), K–H(2B) 3.13(2), K–H(1A') 2.94(3), K–H(1B') 3.23(3), K–H(1C') 2.79(3), K–H(2A'') 2.86(3), K–H(2B'') 3.40(3), K–H(2C'') 2.97(3), K···B(1) 3.315(4), K···B(2) 3.416(4), K···B(1') 3.132(4), K···B(2'') 3.183(4), P–B(1) 1.933(4), P–B(2) 1.949(4), P–C(1) 1.852(3), P–C(8) 1.839(3), K···B(1)···K'' 91.06(9), K···B(2)···K' 88.37(8). Primed and double-primed atoms are related by the screw-axis symmetry operators $x-1/2, 1-y, 1/2-z$ and $x+1/2, 1-y, 1/2-z$, respectively.

alkali metal cations; in the present case these contacts result in oligomerization to afford both dimeric (**15**) and polymeric (**13**) species. The structures of the phosphido-borane anions in these compounds are remarkably similar to that of the anion in the separated ion pair complex **14**, suggesting that coordination of an alkali metal cation has little impact on the bonding within the phosphido-borane anion itself. However, formation of a

separated ion pair results in rapid inversion at the phosphorus center, most likely via a trigonal planar transition state; this behavior is suppressed in the contact ion pair species **13** and **15**.

Addition of a further equivalent of BH_3 to the phosphido-borane salts **13**–**15** yields the corresponding phosphido-bis(borane) complexes **16**–**18**; in spite of the formal analogy between phosphido-bis(borane) anions $\text{R}_2\text{P}(\text{BH}_3)_2^-$ and tetraorganosilanes this ligand class remains largely uninvestigated. The present study reveals that phosphido-bis(borane) anions may adopt a “monodentate” BH_3 -donor mode or a variety of chelating/bridging modes, depending on the nature of the metal center.

The coordination chemistry of phosphido-borane and phosphido-bis(borane) anions is at a very early stage of development, but shows excellent promise for the future. These highly under-utilized ligands, analogues of triorganosilyl anions and tetraorganosilanes, offer an abundance of coordination modes and metal–ligand interactions. We are currently exploring the use of these ligands in main group and lanthanide chemistry.

EXPERIMENTAL SECTION

All manipulations were carried out using standard Schlenk techniques under an atmosphere of dry nitrogen. THF, light petroleum (bp 40–60 °C), toluene, and methylcyclohexane were dried prior to use by distillation under nitrogen from sodium, potassium, or sodium/potassium alloy as appropriate. THF was stored over activated 4A molecular sieves; all other solvents were stored over a potassium film. Deuterated toluene and THF were distilled from potassium, and CDCl_3 was distilled from CaH_2 under nitrogen; all NMR solvents were deoxygenated by three freeze-pump-thaw cycles and were stored over activated 4A molecular sieves. Benzylsodium,²⁶ benzylpotassium,²⁷ and $\{(\text{Me}_3\text{Si})_2\text{CH}\}(\text{Ph})\text{PH}^{12}$ were prepared by previously published procedures; *n*-butyllithium was purchased from Aldrich as a 2.5 M solution in hexanes, and $\text{BH}_3\cdot\text{SMe}_2$ was purchased from Aldrich as a 2.0 M solution in THF. Pmdeta was distilled from CaH_2 under nitrogen and was stored over activated 4A molecular sieves. All other compounds were used as supplied by the manufacturer.

^1H and $^{13}\text{C}\{^1\text{H}\}$ NMR spectra were recorded on a JEOL ECS500 spectrometer operating at 500.16 and 125.65 MHz, respectively, or a Bruker Avance300 spectrometer operating at 300.15 and 75.47 MHz, respectively; chemical shifts are quoted in parts per million (ppm) relative to tetramethylsilane. $^{31}\text{P}\{^1\text{H}\}$, $^{11}\text{B}\{^1\text{H}\}$, and $^7\text{Li}\{^1\text{H}\}$ NMR spectra were recorded on a JEOL ECS500 spectrometer operating at 202.35, 160.16, and 194.38 MHz, respectively; chemical shifts are quoted in ppm relative to external 85% H_3PO_4 , $\text{BF}_3\cdot\text{Et}_2\text{O}$, and 0.1 M LiCl , respectively. Elemental analyses were obtained by the Elemental Analysis Service of London Metropolitan University.

$\{(\text{Me}_3\text{Si})_2\text{CH}\}(\text{Ph})\text{PH}(\text{BH}_3)$ (12**).** To a solution of $\{(\text{Me}_3\text{Si})_2\text{CH}\}(\text{Ph})\text{PH}$ (9.78 g, 36.43 mmol) in THF (20 mL) was added $\text{BH}_3\cdot\text{SMe}_2$ (18.2 mL of a 2.0 M solution in THF, 36.40 mmol). After 1 h stirring the solvent was removed in vacuo to yield a white solid, which was crystallized from cold (–30 °C) THF as colorless blocks. Isolated yield: 8.89 g, 63%. $^1\text{H}\{^{11}\text{B}\}$ NMR (CDCl_3 , 25 °C) δ 0.29 (s, 9H, SiMe_3), 0.36 (s, 9H, SiMe_3), 0.76 (d, $J_{\text{PH}} = 19.3$ Hz, 1H, CHP), 0.94 (dd, $^1J_{\text{PH}} = 15.3$ Hz, $^3J_{\text{HH}} = 6.4$ Hz, 3H, BH_3), 5.72 (dq, $^1J_{\text{PH}} = 368.9$ Hz, $^3J_{\text{HH}} = 6.4$ Hz, 1H, PH), 7.46 (m, 3H, ArH), 0.77 (m, 2H, ArH). $^{13}\text{C}\{^1\text{H}\}$ NMR (CDCl_3 , 25 °C) δ 1.26 (d, $^3J_{\text{PC}} = 2.9$ Hz, SiMe_3), 2.10 (d, $^3J_{\text{PC}} = 2.9$ Hz, SiMe_3), 9.41 (d, $^1J_{\text{PC}} = 3.0$ Hz, CHP), 128.81 (d, $J_{\text{PC}} = 10.5$ Hz, ArC), 129.21 (d, $J_{\text{PC}} = 51.8$ Hz, ArC), 131.29 (d, $J_{\text{PC}} = 2.4$ Hz, ArC), 133.16 (d, $J_{\text{PC}} = 9.6$ Hz, ArC). $^{11}\text{B}\{^1\text{H}\}$ NMR (CDCl_3 , 25 °C): δ –40.6 (d, br, $^1J_{\text{PB}} = 52$ Hz). $^{31}\text{P}\{^1\text{H}\}$ NMR (CDCl_3 , 25 °C): δ –8.6 (q, br, $^1J_{\text{PB}} = 52$ Hz).

$\{[(\text{Me}_3\text{Si})_2\text{CH}\}(\text{Ph})\text{P}(\text{BH}_3)]\text{Li}(\text{THF})_2\}_\infty$ (13**).** To a solution of **12** (0.41 g, 1.26 mmol) in THF (15 mL) was added $^n\text{BuLi}$ (0.5 mL of 2.5 M solution in hexane, 1.25 mmol). After 1 h stirring the solvent was

Table 1. Crystallographic Data

	12	13	14	15	16b	17	18a	18b
formula	$C_{13}H_{32}BPSi_2$	$C_2H_4BLiO_2PSi$	$C_{10}H_3NaO_8^+C_{13}H_{27}BPSi_2^-$	$C_{44}H_{100}B_2K_2N_6P_2Si_4$	$C_{21}H_4B_2LiO_4PSi_2$	$C_{42}H_{92}B_4Na_3O_4P_2Si_4$	$C_{30}H_{68}B_4K_5O_3Si_4$	$C_{21}H_4B_2KO_2PSi_2$
M_w	282.3	432.5	656.7	987.4	478.3	924.7	740.6	478.5
cryst. size (mm)	$0.45 \times 0.20 \times 0.20$	$0.04 \times 0.02 \times 0.02$	$0.10 \times 0.08 \times 0.04$	$0.45 \times 0.18 \times 0.14$	$0.43 \times 0.30 \times 0.30$	$0.40 \times 0.30 \times 0.30$	$0.40 \times 0.30 \times 0.30$	$0.25 \times 0.20 \times 0.20$
cryst. syst.	triclinic	triclinic	monoclinic	triclinic	monoclinic	triclinic	triclinic	orthorhombic
space group	$P\bar{1}$	$P\bar{1}$	$C2/c$	$P\bar{1}$	$P2_1/c$	$P\bar{1}$	$P\bar{1}$	$Pccn$
a (Å)	6.608(4)	6.2819(4)	30.851(8)	9.8704(7)	15.0280(3)	9.661(3)	8.4901(4)	8.6961(3)
b (Å)	8.627(7)	10.6424(7)	11.927(3)	13.1887(10)	12.7789(3)	12.453(2)	9.7266(5)	30.2919(11)
c (Å)	16.504(16)	19.6382(14)	22.254(6)	13.5125(10)	14.9822(3)	12.956(4)	14.6681(7)	23.9712(9)
α (deg)	97.67(8)	96.9636(7)		105.817(7)		85.291(18)	76.367(4)	
β (deg)	93.65(7)	93.8785(8)	114.293(3)	107.826(6)	92.8258(17)	71.807(19)	89.297(4)	
γ (deg)	106.33(7)	101.6636(8)		100.218(7)		81.117(16)	71.341(4)	
V (Å ³)	889.7(12)	1270.56(15)	7476(4)	1544.5(2)	2873.70(11)	1462.0(6)	1112.66(9)	6314.5(4)
Z	2	2	8	1	4	1	1	8
μ (mm ⁻¹)	0.271	0.216	0.191	0.315	1.815	0.204	0.414	0.308
trans. coeff. range	0.888–0.948	0.991–0.996	0.981–0.992	0.871–0.957	0.509–0.612	0.923–0.941	0.852–0.886	0.927–0.941
reflns. measd.	14598	13027	37659	14729	8707	23357	10096	34085
unique reflns.	4039	7013	10809	5946	4451	5118	4636	5552
R_{int}	0.098	0.022	0.042	0.049	0.025	0.085	0.027	0.055
reflns. with $F^2 > 2\sigma$	2496	5706	8422	4816	3928	4089	3377	3579
refined parameters	198	271	397	294	413	292	247	292
R (on F , $F^2 > 2\sigma$) ^a	0.077	0.043	0.040	0.053	0.068	0.051	0.033	0.051
R_w (on F^2 , all data) ^a	0.223	0.123	0.102	0.150	0.196	0.149	0.081	0.140
goodness of fit ^a	1.041	1.031	1.025	1.071	1.066	1.062	0.923	0.987
max. min electron density (e Å ⁻³)	0.58, –0.31	0.60, –0.29	0.37, –0.23	0.64, –0.45	0.91, –0.99	0.41, –0.34	0.37, –0.45	0.54, –0.40

^a $R = \sum ||F_o| - |F_c|| / \sum |F_o|$; $R_w = [\sum w(F_o^2 - F_c^2)^2 / \sum w(F_o^2)]^{1/2}$; $S = [\sum w(F_o^2 - F_c^2)^2 / (\text{no. data} - \text{no. params})]^{1/2}$ for all data.

removed in vacuo to yield an off-white solid. Colorless blocks of **13** suitable for X-ray crystallography were obtained from cold ($-30\text{ }^{\circ}\text{C}$) methylcyclohexane/THF (approx 10:1). Isolated crystalline yield: 0.34 g, 63%. Anal. Calcd for $[[\{(Me_3Si)_2CH\}(Ph)P(BH_3)]Li(THF)_2]_{\infty}$: C 58.32, H 10.02%. Found C 58.29, H 9.95%. $^1H\{^{11}B\}$ NMR (d_8 -toluene, $25\text{ }^{\circ}\text{C}$): δ 0.29 (s, 9H, SiMe₃), 0.39 (s, 9H, SiMe₃), 0.63 (d, $^2J_{PH} = 7.8$ Hz, 1H, CHP), 1.04 (s, 3H, BH₃), 1.40 (m, 8H, THF), 3.54 (m, 8H, THF), 6.99 (m, 1H, ArH), 7.17 (m, 2H, ArH), 7.78 (m, 2H, ArH). $^{13}C\{^1H\}$ NMR (d_8 -toluene, $25\text{ }^{\circ}\text{C}$): δ 2.29 (d, $^3J_{PC} = 7.7$ Hz, SiMe₃), 3.32 (SiMe₃), 8.86 (d, $^1J_{PC} = 34.6$ Hz, CHP), 25.12 (THF), 68.13 (THF), 124.23 (ArC), 127.14 (d, $^1J_{PC} = 4.8$ Hz, ArC), 131.84 (d, $J_{PC} = 11.5$ Hz, ArC), 149.62 (d, $J_{PC} = 16.3$ Hz, ArC). $^{11}B\{^1H\}$ NMR (d_8 -toluene, $25\text{ }^{\circ}\text{C}$): δ -32.7 (d, br, $^1J_{BP} = 44$ Hz). $^{31}P\{^1H\}$ NMR (d_8 -toluene, $25\text{ }^{\circ}\text{C}$): δ -56.8 (q, br, $^1J_{PB} = 44$ Hz). $^7Li\{^1H\}$ NMR (d_8 -toluene, $25\text{ }^{\circ}\text{C}$): δ 3.1.

$[[\{(Me_3Si)_2CH\}(Ph)P(BH_3)]Na(12\text{-crown-4})_2]$ (**14**). To a solution of **12** (0.37 g, 1.31 mmol) in THF (10 mL) was added, dropwise, a solution of benzylsodium (0.15 g, 1.31 mmol) in THF (20 mL), and this mixture was stirred for 1 h. 12-crown-4 (0.4 mL, 2.62 mmol) was added to the solution, and this mixture was stirred for 10 min. Solvent was removed in vacuo to give a pale yellow solid, which was crystallized from cold ($-30\text{ }^{\circ}\text{C}$) toluene/THF (approx 10:1) as colorless crystals suitable for X-ray crystallography. Isolated crystalline yield: 0.73 g, 86%. Anal. Calcd for $[[\{(Me_3Si)_2CH\}(Ph)P(BH_3)]Na(12\text{-crown-4})_2]$: C 53.48, H 8.96%. Found C 53.04, H 9.06%. $^1H\{^{11}B\}$ NMR (d_8 -THF, $25\text{ }^{\circ}\text{C}$): δ -0.05 (s, br, 9H, SiMe₃), 0.14 (s, br, 9H, SiMe₃), 0.20 (d, $^2J_{PH} = 5.5$ Hz, 1H, CHP), 0.97 (d, $^2J_{PH} = 4.1$ Hz, 3H, BH₃), 3.63 (s, 32H, 12-crown-4), 6.70 (m, 1H, ArH), 6.91 (m, 2H, ArH), 7.55 (m, 2H, ArH). $^{13}C\{^1H\}$ NMR (d_8 -THF, $25\text{ }^{\circ}\text{C}$): δ 1.81 (s, br, SiMe₃), 2.91 (s, br, SiMe₃), 10.51 (d, $^1J_{PC} = 47.9$ Hz, CHP), 66.13 (12-crown-4), 121.11, 125.73 (ArC), 131.84 (d, $J_{PC} = 11.5$ Hz, ArC), 157.07 (d, $J_{PC} = 35.5$ Hz, ArC). $^{11}B\{^1H\}$ NMR (d_8 -THF, $25\text{ }^{\circ}\text{C}$): δ -32.4 (s, br). $^{31}P\{^1H\}$ NMR (d_8 -THF, $25\text{ }^{\circ}\text{C}$): δ -41.0 (d, br, $^1J_{PB} = 26$ Hz).

$[[\{(Me_3Si)_2CH\}(Ph)P(BH_3)]K(pmdeta)]_2$ (**15**). To a solution of **12** (0.45 g, 1.59 mmol) in THF (15 mL) was added a solution of benzylpotassium (0.21 g, 1.59 mmol) in THF (10 mL). After 1 h stirring the solvent was removed in vacuo, yielding an orange powder. The product was dissolved in toluene (20 mL), and pmdeta (0.3 mL, 1.44 mmol) was added. The solvent volume was then carefully reduced in vacuo until the product began to precipitate. The turbid solution was warmed slightly to dissolve the product, and upon cooling to $-30\text{ }^{\circ}\text{C}$ colorless crystals of **15** suitable for X-ray crystallography were deposited. Isolated crystalline yield: 0.46 g, 59%. Anal. Calcd for $[[\{(Me_3Si)_2CH\}(Ph)P(BH_3)]K(pmdeta)]_2$: C 53.52, H 10.21, N 8.51%. Found C 53.41, H 10.14, N 8.42%. $^1H\{^{11}B\}$ NMR (d_8 -toluene, $25\text{ }^{\circ}\text{C}$): δ 0.28 (s, 9H, SiMe₃), 0.42 (s, 9H, SiMe₃), 0.61 (d, $^2J_{PH} = 6.9$ Hz, 1H, CHP), 1.08 (d, $^2J_{PH} = 4.1$ Hz, 3H, BH₃), 1.93 (m, 4H, NCH₂), 1.95 (m, 4H, NCH₂), 1.99 (s, 3H, NMe), 2.09 (s, 12H, NMe₂), 6.98 (m, 1H, ArH), 7.20 (m, 2H, ArH), 7.80 (m, 2H, ArH). $^{13}C\{^1H\}$ NMR (d_8 -toluene, $25\text{ }^{\circ}\text{C}$): δ 2.25 (d, $^3J_{PC} = 7.7$ Hz, SiMe₃), 3.20 (SiMe₃), 9.78 (d, $^1J_{PC} = 43.1$ Hz, CHP), 41.00 (NMe), 44.80 (NMe₂), 55.60 (NCH₂), 56.76 (NCH₂), 123.42 (ArC), 127.09 (d, $J_{PC} = 2.9$ Hz, ArC), 131.83 (d, $J_{PC} = 11.5$ Hz, ArC), 153.07 (d, $J_{PC} = 25.9$ Hz). $^{11}B\{^1H\}$ NMR (d_8 -toluene, $25\text{ }^{\circ}\text{C}$): δ -31.6 (d, br, $^1J_{BP} = 20$ Hz). $^{31}P\{^1H\}$ NMR (d_8 -toluene, $25\text{ }^{\circ}\text{C}$): δ -50.6 (d, br, $^1J_{PB} = 20$ Hz).

$[[\{(Me_3Si)_2CH\}(Ph)P(BH_3)]Li(12\text{-crown-4})]$ (**16b**). To a solution of **12** (0.54 g, 1.91 mmol) in THF (10 mL) was added n -BuLi (0.8 mL of a 2.5 M solution in hexane, 2.0 mmol). This mixture was stirred for 1 h and then a solution of BH₃·SMe₂ (1.0 mL, of a 2.0 M solution in THF, 2.0 mmol) was added. This mixture was stirred for a further 1 h and then the solvent was removed in vacuo to yield a colorless solid. The product was dissolved in toluene (5 mL), and 12-crown-4 (0.3 mL, 1.85 mmol) was added. Colorless crystals of **16b** suitable for X-ray crystallography were obtained upon cooling this solution to $5\text{ }^{\circ}\text{C}$ for 16 h. Isolated crystalline yield: 0.70 g, 77%. Anal. Calcd for $[[\{(Me_3Si)_2CH\}(Ph)P(BH_3)]Li(12\text{-crown-4})]$: C 52.73, H 9.69%. Found C 52.67, H 9.81%. $^1H\{^{11}B\}$ NMR (d_8 -THF, $25\text{ }^{\circ}\text{C}$): δ -0.05 (s, 18H, SiMe₃), 0.57 (d, $^2J_{PH} = 13.8$ Hz, 1H, CHP), 0.77 (d, $^2J_{PH} = 10.1$ Hz, 6H, BH₃), 3.75 (s, 16H, 12-crown-4), 7.07 (m, 2H, ArH),

7.12 (m, 2H, ArH), 7.79 (m, 1H, ArH). $^{13}C\{^1H\}$ NMR (d_8 -THF, $25\text{ }^{\circ}\text{C}$): δ 3.20 (SiMe₃), 11.85 (d, $^1J_{PC} = 6.7$ Hz, CHP), 67.15 (12-crown-4), 126.02 (ArC), 126.31 (d, $J_{PC} = 7.7$ Hz, ArC), 132.32 (d, $J_{PC} = 6.7$ Hz, ArC), 146.78 (d, $J_{PC} = 29.7$ Hz, ArC). $^{11}B\{^1H\}$ NMR (d_8 -THF, $25\text{ }^{\circ}\text{C}$): δ -32.5 (d, br, $^1J_{BP} = 46$ Hz). $^{31}P\{^1H\}$ NMR (d_8 -THF, $25\text{ }^{\circ}\text{C}$): δ -8.8 (br). $^7Li\{^1H\}$ NMR (d_8 -THF, $25\text{ }^{\circ}\text{C}$): δ -0.7.

$[[\{(Me_3Si)_2CH\}(Ph)P(BH_3)]Na(THF)_2]$ (**17**). To a solution of **12** (0.45 g, 1.59 mmol) in THF (10 mL) was added a solution of benzylsodium (184 mg, 1.61 mmol). This mixture was stirred for 1 h and then a solution of BH₃·SMe₂ (0.8 mL, of a 2.0 M solution in THF, 1.60 mmol) was added. This mixture was stirred for a further 1 h and then the solvent was removed in vacuo to yield a colorless solid. Single crystals suitable for X-ray crystallography were obtained from a cold ($-30\text{ }^{\circ}\text{C}$) mixture of methylcyclohexane (10 mL), toluene (2 mL), and THF (5 mL). Isolated crystalline yield: 0.46 g, 63%. Anal. Calcd for $[[\{(Me_3Si)_2CH\}(Ph)P(BH_3)]Na(THF)_2]$: C 54.55, H 10.03%. Found C 54.25, H 9.65%. $^1H\{^{11}B\}$ NMR (d_8 -THF, $25\text{ }^{\circ}\text{C}$): δ 0.07 (s, 18H, SiMe₃), 0.63 (d, $^2J_{PH} = 8.7$ Hz, 6H, BH₃), 0.64 (d, $^2J_{PH} = 15.1$ Hz, 1H, CHP), 1.78 (m, 8H, THF), 3.61 (m, 8H, THF), 7.12 (m, 1H, ArH), 7.17 (m, 2H, ArH), 7.74 (m, 2H, ArH). $^{13}C\{^1H\}$ NMR (d_8 -THF, $25\text{ }^{\circ}\text{C}$): δ 2.79 (d, $^3J_{PC} = 1.9$ Hz, SiMe₃), 10.55 (d, $^1J_{PC} = 2.9$ Hz, CHP), 25.30 (THF), 67.14 (THF), 126.58 (ArC), 126.68 (d, $J_{PC} = 7.7$ Hz, ArC), 132.03 (d, $J_{PC} = 7.7$ Hz, ArC), 143.84 (d, $J_{PC} = 36.4$ Hz, ArC). $^{11}B\{^1H\}$ NMR (d_8 -THF, $25\text{ }^{\circ}\text{C}$): δ -33.8 (d, br, $^1J_{BP} = 69$ Hz). $^{31}P\{^1H\}$ NMR (d_8 -THF, $25\text{ }^{\circ}\text{C}$): δ -14.9 (br).

$[[\{(Me_3Si)_2CH\}(Ph)P(BH_3)]K(THF)_{0.5}]_{\infty}$ (**18a**). To a solution of **12** (0.42 g, 1.49 mmol) in THF (10 mL) was added a solution of benzylpotassium (194 mg, 1.49 mmol) in THF (10 mL). This mixture was stirred for 1 h and then a solution of BH₃·SMe₂ (0.8 mL of a 2.0 M solution in THF, 1.60 mmol) was added. The solution was stirred for a further 1 h and then the solvent was removed in vacuo to yield a colorless solid. Colorless crystals suitable of **18a** for X-ray crystallography were obtained from cold ($5\text{ }^{\circ}\text{C}$) toluene/THF. A second batch of crystals, isolated in a similar manner, proved to be of the alternate solvate $[[\{(Me_3Si)_2CH\}(Ph)P(BH_3)]K(THF)_2]_{\infty}/2PhMe]$ (**18b**), which was characterized solely by X-ray crystallography. The following data refer to **18a**. Isolated crystalline yield: 0.48 g, 88%. Anal. Calcd for $[[\{(Me_3Si)_2CH\}(Ph)P(BH_3)]K(THF)_{0.5}]_{\infty}$: C 48.65, H 9.25%. Found C 48.71, H 9.05%. $^1H\{^{11}B\}$ NMR (d_8 -THF, $25\text{ }^{\circ}\text{C}$): δ 0.07 (s, 18H, SiMe₃), 0.62 (d, $^2J_{PH} = 14.7$ Hz, 1H, CHP), 0.70 (d, $^2J_{PH} = 9.6$ Hz, 6H, BH₃), 1.78 (m, 8H, THF), 3.62 (m, 8H, THF), 7.10 (m, 1H, ArH), 7.14 (m, 2H, ArH), 7.77 (m, 2H, ArH). $^{13}C\{^1H\}$ NMR (d_8 -THF, $25\text{ }^{\circ}\text{C}$): δ 2.91 (d, $J_{PC} = 1.9$ Hz, SiMe₃), 11.37 (d, $J_{PC} = 3.8$ Hz, CHP), 25.01 (THF), 66.85 (THF), 126.38, 126.46 (ArC), 132.27 (d, $^3J_{PC} = 6.7$ Hz, ArC), 144.58 (d, $J_{PC} = 34.5$ Hz, ArC). $^{11}B\{^1H\}$ NMR (d_8 -THF, $25\text{ }^{\circ}\text{C}$): δ -32.9 (d, br, $^1J_{BP} = 64$ Hz). $^{31}P\{^1H\}$ NMR (d_8 -THF, $25\text{ }^{\circ}\text{C}$): δ -14.1 (br).

Crystal Structure Determinations of 12–18. For **12**, **14**, **15**, **16b**, **17**, **18a**, and **18b** measurements were made at 150 K on an Oxford Diffraction (Agilent Technologies) Gemini A Ultra diffractometer or a Nonius KappaCCD diffractometer, using MoK α radiation ($\lambda = 0.71073\text{ \AA}$); for **13** measurements were made at 120 K using synchrotron radiation ($\lambda = 0.6941\text{ \AA}$). Cell parameters were refined from the observed positions of all strong reflections. Intensities were corrected semi-empirically for absorption, based on symmetry-equivalent and repeated reflections. The structures were solved by direct methods and refined on F^2 values for all unique data. Table 1 gives further details. All non-hydrogen atoms were refined anisotropically, and C-bound H atoms were constrained with a riding model, while B-bound H atoms were freely refined; $U(H)$ was set at 1.2 (1.5 for methyl groups) times U_{eq} for the parent C atom. Disorder in one SiMe₃ group of **12** was successfully modeled with both components refined freely; the disordered crown ligand of **16b** was refined with the aid of restraints on geometry and displacement parameters, and the same applies to the disordered THF of **18a**. Highly disordered solvent in **18b** could not be modeled with discrete atoms and was treated by the SQUEEZE procedure of PLATON;²⁸ while the volume of the disorder region is appropriate for toluene (approximately half a molecule per potassium ion), the electron density calculated in this region is anomalously low, suggesting that the solvent is readily lost

from the crystals before diffraction data collection. Other programs were Oxford Diffraction CrysAlisPro, Nonius COLLECT/EvalCCD and Bruker APEX2 for data collection and processing, and SHELXTL for structure solution, refinement, and molecular graphics.²⁹

■ ASSOCIATED CONTENT

■ Supporting Information

For 12–15, 16b, 17, 18a, and 18b details of structure determination, atomic coordinates, bond lengths and angles, and displacement parameters in CIF format. This material is available free of charge via the Internet at <http://pubs.acs.org>.

■ AUTHOR INFORMATION

Corresponding Author

*E-mail: k.j.izod@ncl.ac.uk

Notes

The authors declare no competing financial interest.

■ ACKNOWLEDGMENTS

The authors are grateful to the EPSRC and Newcastle University for financial support, EPSRC also for funding the U.K. National Crystallography Service and STFC for access to synchrotron facilities at SRS Daresbury Laboratory.

■ REFERENCES

- (1) (a) Gaumont, A.-C.; Hursthouse, M. B.; Coles, S. J.; Brown, J. M. *Chem. Commun.* **1999**, 63. (b) Pican, S.; Gaumont, A.-C. *Chem. Commun.* **2005**, 2393.
- (2) (a) Jaska, A. C.; Lough, A. J.; Manners, I. *Dalton Trans.* **2005**, 326. (b) Lee, K.; Clark, T. J.; Lough, A. J.; Manners, I. *Dalton Trans.* **2008**, 2732. (c) Jaska, C. A.; Dorn, H.; Lough, A. J.; Manners, I. *Chem.—Eur. J.* **2003**, 9, 271.
- (3) Abdellah, I.; Bernoud, E.; Lohier, J.-F.; Alayrac, C.; Toupet, L.; Lepetit, C.; Gaumont, A.-C. *Chem. Commun.* **2012**, 48, 4088.
- (4) (a) Müller, G.; Brand, J. *Organometallics* **2003**, 22, 1463. (b) Dornhaus, F.; Bolte, M.; Lerner, H.-W.; Wagner, M. *Eur. J. Inorg. Chem.* **2006**, 1777. (c) Dornhaus, F.; Bolte, M.; Lerner, H.-W.; Wagner, M. *Eur. J. Inorg. Chem.* **2006**, 5138.
- (5) (a) Dornhaus, F.; Bolte, M.; Lerner, H.-W.; Wagner, M. *J. Organomet. Chem.* **2007**, 692, 2949. (b) Kückmann, T. I.; Dornhaus, F.; Bolte, M.; Lerner, H.-W.; Holthausen, M. C.; Wagner, M. *Eur. J. Inorg. Chem.* **2007**, 1989.
- (6) Consiglio, G. B.; Queval, P.; Harrison-Marchand, A.; Mordini, A.; Lohier, J.-F.; Delacroix, O.; Gaumont, A.-C.; Gérard, H.; Maddaluno, J.; Oulyadi, H. *J. Am. Chem. Soc.* **2011**, 133, 6472.
- (7) Dornhaus, F.; Bolte, M. *Acta Crystallogr.* **2006**, E62, m3573.
- (8) Rudzевич, V. L.; Gornitzka, H.; Romanenko, V. D.; Bertrand, G. *Chem. Commun.* **2001**, 1634.
- (9) Fuller, A. M.; Mountford, A. J.; Scott, M. L.; Coles, S. J.; Horton, P. N.; Hughes, D. L.; Hursthouse, M. B.; Lancaster, S. J. *Inorg. Chem.* **2009**, 48, 11474.
- (10) Izod, K.; Watson, J. M.; Clegg, W.; Harrington, R. W. *Dalton Trans.* **2011**, 40, 11712.
- (11) Izod, K.; Watson, J. M.; Clegg, W.; Harrington, R. W. *Eur. J. Inorg. Chem.* **2012**, 1696.
- (12) (a) Izod, K.; Stewart, J.; Clark, E. R.; Clegg, W.; Harrington, R. W. *Inorg. Chem.* **2010**, 49, 4698. (b) Appel, R.; Peters, J.; Schmitz, R. Z. *Anorg. Allg. Chem.* **1981**, 475, 18.
- (13) (a) Bent, H. A. *J. Chem. Phys.* **1959**, 33, 1260. (b) Bent, H. A. *Chem. Rev.* **1961**, 61, 275. (c) Hugheey, J. E. *Inorg. Chem.* **1981**, 20, 4033.
- (14) Imamoto, T.; Oshiki, T.; Onozawa, T.; Kusumoto, T.; Sato, K. *J. Am. Chem. Soc.* **1990**, 112, 5244.
- (15) Loschen, C.; Voigt, K.; Frunzke, J.; Diefenbach, A.; Diedenhofen, M.; Frenking, G. Z. *Anorg. Allg. Chem.* **2002**, 682, 1294.
- (16) (a) Kapp, J.; Schade, C.; El-Nahasa, A. M.; Schleyer, P. von R. *Angew. Chem., Int. Ed. Engl.* **1996**, 35, 2236. (b) Dixon, D. A.; Arduengo, A. J., III; Fukunaga, T. *J. Am. Chem. Soc.* **1986**, 108, 2461. (c) Dixon, D. A.; Arduengo, A. J., III *J. Chem. Soc. Chem. Commun.* **1987**, 498. (d) Dixon, D. A.; Arduengo, A. J., III *J. Am. Chem. Soc.* **1987**, 109, 338. (e) Schwerdtfeger, P.; Laakkonen, L. J.; Pyykkö, P. *J. Chem. Phys.* **1992**, 96, 6807. (f) Schwerdtfeger, P.; Hunt, P. *Adv. Mol. Struct. Res.* **1999**, 5, 223. (g) Schwerdtfeger, P.; Boyd, P. D. W.; Fischer, T.; Hunt, P.; Liddell, M. *J. Am. Chem. Soc.* **1994**, 116, 9620. (h) Göller, A.; Clark, T. *Chem. Commun.* **1997**, 1033.
- (17) (a) Beachler, R. D.; Casey, J. P.; Cook, R. J.; Senkler, G. H., Jr.; Mislow, K. *J. Am. Chem. Soc.* **1987**, 109, 338. (b) Beachler, R. D.; Mislow, K. *J. Am. Chem. Soc.* **1971**, 93, 773. (c) Beachler, R. D.; Andose, J. D.; Stackhouse, J.; Mislow, K. *J. Am. Chem. Soc.* **1972**, 94, 8060. (d) Driess, M.; Merz, K.; Monse, C. Z. *Anorg. Allg. Chem.* **2000**, 626, 2264.
- (18) (a) Izod, K.; McFarlane, W.; Allen, B.; Clegg, W.; Harrington, R. W. *Organometallics* **2005**, 24, 2157. (b) Izod, K.; Stewart, J.; Clark, E. R.; McFarlane, W.; Allen, B.; Clegg, W.; Harrington, R. W. *Organometallics* **2009**, 28, 3327.
- (19) Izod, K.; Clark, E. R.; Stewart, J. *Inorg. Chem.* **2011**, 50, 3651.
- (20) Izod, K. *Adv. Inorg. Chem.* **2000**, 50, 33.
- (21) For examples see: (a) Wiberg, N.; Neidermayer, W.; Nöth, H.; Warchold, M. *J. Organomet. Chem.* **2001**, 628, 46. (b) Bravo-Zhivotovskii, D.; Molev, G.; Kravchenko, V.; Botoshansky, M.; Schmidt, A.; Apeloig, Y. *Organometallics* **2006**, 25, 4719. (c) Strohmman, C.; Däschlein, C. *Chem. Commun.* **2008**, 2791. (d) Sekiguchi, A.; Nanjo, M.; Kabuto, C.; Sakurai, H. *Organometallics* **1995**, 14, 2630. (e) Teclé, B.; Ilsley, W. H.; Oliver, J. P. *Organometallics* **1982**, 1, 875. (f) Sekiguchi, A.; Nanjo, M.; Kabuto, C.; Sakurai, H. *Angew. Chem., Int. Ed. Engl.* **1997**, 36, 113.
- (22) Nöth, H.; Thomas, S. *Eur. J. Inorg. Chem.* **1999**, 1373.
- (23) (a) Kim, D. Y.; Girolami, G. S. *Inorg. Chem.* **2010**, 49, 4924. (b) Daly, S. R.; Girolami, G. S. *Inorg. Chem.* **2010**, 49, 5157. (c) Daly, S. R.; Girolami, G. S. *Chem. Commun.* **2010**, 46, 407. (d) Daly, S. R.; Girolami, G. S. *Inorg. Chem.* **2010**, 49, 4578. (e) Daly, S. R.; Bellot, B. J.; Kim, D. Y.; Girolami, G. S. *J. Am. Chem. Soc.* **2010**, 132, 7254. (f) Daly, S. R.; Kim, D. Y.; Yang, Y.; Abelson, J. R.; Girolami, G. S. *J. Am. Chem. Soc.* **2010**, 132, 2106.
- (24) Ruiz, J. C. G.; Nöth, H.; Warchold, M. *Eur. J. Inorg. Chem.* **2008**, 251.
- (25) Giese, H.-H.; Habereeder, T.; Nöth, H.; Ponikvar, W.; Thomas, S.; Warchold, M. *Inorg. Chem.* **1999**, 38, 4188.
- (26) Bertz, S. H.; Gibson, C. P.; Dabbagh, G. *Organometallics* **1988**, 7, 227.
- (27) Lochmann, L.; Trekoval, J. *J. Organomet. Chem.* **1987**, 326, 1.
- (28) Spek, A. L. *Acta Crystallogr., Sect. D* **2009**, 65, 148.
- (29) (a) CrysAlisPro; Oxford Diffraction Ltd (now part of Agilent Technologies Ltd): Oxford, U.K., 2008; (b) COLLECT; Nonius BV: Delft, The Netherlands, 1998; (c) Duisenberg, A. J. M.; Kroon-Batenburg, L. M. J.; Schreurs, A. M. M. *J. Appl. Crystallogr.* **2003**, 36, 220. (d) APEX2; Bruker AXS Inc.: Madison, WI, 2010; (e) Sheldrick, G. M. *Acta Crystallogr., Sect. A* **2008**, 64, 112.